agronomy

MDPI

*Article*

# Optimizing Canopy Architecture Synergizes Yield and Quality: A Comprehensive Evaluation of Sugar Beet Germplasm During the Taproot Expansion Stage

**Rongzhen Suo, Ruili Wang, Yue Li, Zhimin Yang * and Ke Shao ***

Institute of Biotechnology, Inner Mongolia Academy of Science and Technology, Hohhot 010010, China; suorongzhen@outlook.com (R.S.); 96048@126.com (R.W.); m15848083400@163.com (Y.L.)
* Correspondence: yzm0110@126.com (Z.Y.); shaoke141202608@163.com (K.S.)

**Abstract**

The negative relationship between root yield and sugar content remains an important challenge for sugar beet (*Beta vulgaris* L.) improvement. Optimizing canopy architecture may provide an effective strategy for identifying germplasm with favorable combinations of productivity and quality. In this study, 216 sugar beet accessions were evaluated under a single planting configuration at the Liangcheng Experimental Station, Inner Mongolia, China. Eleven quantitative traits related to canopy architecture, yield, and quality were measured during the taproot expansion stage. Root yield was negatively correlated with sugar content. By integrating Spearman correlation analysis with Random Forest (RF) regression, five complementary indicators, including canopy width, SPAD, leaf length, plant height, and lower leaf angle, were retained for multi-trait evaluation. Principal Component Analysis and Ward's hierarchical clustering further classified the accessions into High-Yield, High-Sugar, and Balanced phenotypic typologies with distinct combinations of yield, sugar content, and canopy traits. A performance-adjusted RF-TOPSIS framework was subsequently used to rank the 216 accessions. BV82 achieved the highest relative closeness coefficient, and all top 20 accessions belonged to the High-Yield group. Sensitivity analyses indicated that the overall ranking was generally stable under alternative weighting schemes and moderate perturbations of criterion weights. These results provide candidate canopy traits and germplasm resources for further field validation and sugar beet breeding.

**Keywords:** *Beta vulgaris* L.; phenotypic evaluation; canopy architecture; random forest; TOPSIS model

Check for updates

Academic Editor: Carlo Leifert

Received: 19 August 2026
Revised: 3 October 2026
Accepted: 4 October 2026
Published: 7 October 2026

**Copyright:** © 2026 by the authors. Licensee MDPI, Basel, Switzerland. This article is an open access article distributed under the terms and conditions of the Creative Commons Attribution (CC BY) license.

## 1. Introduction

Meeting the growing global demand for agricultural products while limiting further expansion of cropland requires sustained improvements in crop productivity on existing agricultural land [1]. Plant density is a key determinant of sugar beet canopy development and productivity, influencing canopy closure, leaf area development, and yield formation [2–4]. Increasing plant populations can accelerate canopy establishment and improve sugar yield within an appropriate density range, whereas excessive density may intensify interplant competition and constrain individual plant growth, indicating an agronomic optimum rather than a simple linear response [2–4]. Beyond plant density itself, optimizing the spatial organization of foliage provides an additional opportunity to improve canopy performance, as exemplified by the recently proposed maize "smart canopy", in which

vertically differentiated leaf angles improve canopy light distribution, photosynthetic performance, and yield under high-density conditions [5]. In sugar beet (*Beta vulgaris* L.), canopy optimization is particularly important because yield formation depends strongly on timely canopy development, efficient interception and utilization of incident radiation, and the subsequent partitioning of assimilates to the storage root [2,6,7]. Recent field experiments combined with a synthesis of six decades of plant-density studies showed that increasing sugar beet plant populations accelerated canopy closure and increased sugar yield up to an agronomically optimal density [2]. Moreover, substantial genotypic variation exists in sugar beet canopy architecture, including differences in leaf and petiole orientation, canopy expansion, and three-dimensional foliage distribution, with measurable consequences for light interception, radiation use efficiency, biomass partitioning, and sugar yield [6,7]. Collectively, these findings suggest that improving sugar beet productivity under intensive cultivation requires not simply increasing plant density or modifying individual architectural traits, but identifying canopy configurations that effectively coordinate individual plant architecture with population-level resource capture.

In sugar beet, such coordination is determined by multiple architectural traits that collectively define the three-dimensional distribution of photosynthetic surfaces. Plant height and canopy width determine the vertical and horizontal extent of the canopy, whereas leaf and petiole inclination regulate foliage orientation and light penetration [6,8]. Consequently, canopy performance depends not only on the amount of foliage produced but also on its spatial arrangement and the resulting efficiency of radiation capture and utilization [7–10]. Early and rapid canopy development increases seasonal radiation interception and dry matter production, whereas differences in canopy angle further modify canopy closure, leaf area index, and radiation use efficiency [7,11,12]. Notably, intermediate sugar beet canopy types have achieved greater sugar yield than either upright or prostrate types, while upright canopies can maintain relatively high radiation use efficiency later in the season [7]. These findings indicate that productive canopy architecture cannot be defined by maximizing a single structural trait but instead depends on the coordinated expression of multiple architectural characteristics.

The agronomic value of canopy optimization ultimately depends on how efficiently captured radiation is converted into biomass and subsequently partitioned to the storage root. Historical improvements in sugar beet productivity have involved both enhanced resource capture and a shift in assimilate partitioning from leaf and structural biomass toward sucrose storage in the taproot [11,12]. However, sugar yield is not determined by canopy assimilation alone because storage-root productivity also depends on sink strength and the capacity of taproot tissues to import and store assimilates [12–14]. Experimental evidence shows that elevated cell turgor can inhibit sucrose uptake in sugar beet taproot tissue [13], while variation in root-to-shoot partitioning among contrasting canopy types is associated with differences in sugar yield [7]. Importantly, substantial phenotypic variation in plant architecture exists among sugar beet germplasms, including differences in plant type, plant height, petiole characteristics, and three-dimensional canopy structure [6,15]. Such variation provides an important resource for crop improvement because architectural differences can modify canopy light interception, radiation use efficiency, biomass partitioning, and ultimately sugar yield [6,7,11]. Therefore, characterizing multidimensional architectural variation and identifying favorable trait combinations are important for screening elite germplasm and parental materials with improved canopy performance and yield potential.

Despite increasing evidence for the importance of canopy architecture in sugar beet, the identification of favorable plant types remains challenging because agronomic performance reflects the coordinated effects of multiple architectural traits rather than any

single characteristic [6,7]. Although substantial phenotypic diversity has been documented across sugar beet germplasm [6,15], comparatively limited attention has been given to integrating multidimensional canopy traits to distinguish contrasting plant architectures and identify germplasms combining desirable canopy characteristics with superior yield and quality. Addressing this gap requires systematic evaluation of architectural variation across diverse germplasm resources to support the identification of elite plant types and potential parental materials.

Therefore, this study utilized 216 sugar beet germplasms of diverse geographic origins to characterize phenotypic variation in multidimensional canopy architectural traits during the taproot expansion stage. We aimed to identify favorable architectural trait combinations associated with yield and quality and to establish a comprehensive evaluation framework for screening elite germplasm and potential parental materials. The results are expected to provide a phenotypic basis for plant architecture improvement and the selection of sugar beet germplasm with favorable canopy characteristics for subsequent field evaluation.

## 2. Materials and Methods

### *2.1. Plant Materials*

A diverse panel consisting of 216 sugar beet (*Beta vulgaris* L.) accessions was assembled for this study. The collection represents a broad geographic distribution, including germplasm from the Netherlands (77), China (67), Germany (37), the United Kingdom (14), the United States (10), Switzerland (4), and Russia (1). Additionally, six space-induced mutant lines were included to expand the genetic variation. Detailed information about these accessions is provided in Supplementary Materials.

### *2.2. Experimental Site and Design*

The field experiment was conducted during the 2025 growing season at the Liangcheng Experimental Station, Inner Mongolia, China (40°30′05″ N, 112°08′49″ E), a region characterized by a cold and arid mesothermal continental climate, with a long-term mean annual temperature of 4.5 °C and mean annual precipitation of 376.1 mm. In contrast to the long-term climatic conditions, 2025 was an exceptionally wet year, with a mean annual temperature of approximately 7.1 °C and annual precipitation of approximately 2918.9 mm. The frost-free period is approximately 120 days. The experimental soil was chestnut soil, and the baseline physicochemical properties of the 0–20 cm soil layer prior to sowing are presented in Table 1.

**Table 1.** Baseline physicochemical properties of the soil (0–20 cm depth) in the experimental field.

| Plot | pH | P (mg kg$^{-1}$) | K (g kg$^{-1}$) | SOC (%) | SWC (%) | $NH_4^+$-N (mg kg$^{-1}$) | $NO_3^-$-N (mg kg$^{-1}$) |
|---|---|---|---|---|---|---|---|
| plot 1 | 8.06 | 69.1 | 0.48 | 1.78 | 12.79 | 14.76 | 23.22 |
| plot 2 | 8.05 | 79.4 | 0.35 | 1.87 | 7.73 | 13.54 | 30.08 |
| plot 3 | 8.17 | 81.5 | 0.46 | 2.11 | 13.01 | 19.70 | 21.82 |

Note: P, phosphorus; K, potassium; SOC, soil organic carbon; SWC, soil water content; $NH_4^+$-N, ammonium nitrogen; $NO_3^-$-N, nitrate nitrogen.

Before sowing, the field was rotary-tilled to a depth of approximately 20 cm, and diammonium phosphate was applied as basal fertilizer at a rate of 525 kg ha$^{-1}$, following local agronomic practice. Drip irrigation was used throughout the growing season, with the same irrigation management applied uniformly to all experimental plots. The experiment was conducted on flat ground and arranged in a randomized complete block design (RCBD) with three replicates. Each experimental plot measured 1.2 m × 2.3 m and comprised four

rows of 10 plants, with 0.25 m between plants, 0.40 m between rows, and 0.50 m between adjacent plots. All 216 sugar beet germplasms were grown during the same experimental period and were sown simultaneously on 24 May 2025 at a depth of approximately 3 cm. Seedlings were thinned on 30 June 2025 to maintain the target plant spacing and a uniform stand density. Standard agronomic management practices were applied uniformly to all plots throughout the experimental period.

### *2.3. Data Collection and Phenotypic Evaluation*

Phenotypic data were collected at 83 days after sowing (DAS), corresponding to the taproot expansion stage. Four plants were randomly selected from the two interior rows of each plot for phenotypic measurements, while the two outer rows were excluded to minimize edge effects. Plant height was measured from the base to the highest leaf tip using a measuring tape. Canopy width was measured using a measuring tape and calculated as the average of two perpendicular canopy diameters. The fully expanded leaf number per plant was counted manually. Leaf length and leaf width were measured on the fourth through sixth basal leaves using a ruler. Leaf inclination angles were quantified using a digital protractor (Model LF, Deqing Shengtai Xin Electronic Technology Co., Ltd., Huzhou, China, angular range: 0–360°) by measuring the angle between the petiole and a vertical ground axis. Upper leaf angle and lower leaf angle were evaluated on the fourth through eighth leaves from the canopy apex and base, respectively. SPAD values were measured on the fourth fully expanded leaf from the canopy apex using a SPAD-502 Plus meter (KonicaMinoltaInc., Tokyo, Japan), with three readings taken per leaf and averaged.

For yield and quality evaluation, five plants were harvested from the interior rows of each plot at 123 DAS. After harvest, the shoots were separated from the taproots, and adhering soil and fine roots were carefully removed from the taproot surface. Shoot and taproot fresh weights were measured separately using an electronic balance (ACS-30, Kaifeng Group Co., Ltd., Jinhua, China) to determine biomass and root yield, and the root-to-shoot ratio (R/S ratio) was subsequently calculated. Sugar content was measured using a PAL-1 digital refractometer (ATAGO Co., Ltd., Tokyo, Japan, ranging from 0.0 to 53.0 percent).

### *2.4. Statistical Analysis and Comprehensive Evaluation*

#### 2.4.1. Descriptive Statistics and Genetic Diversity Analysis

Descriptive statistics, including mean, standard deviation (SD), range, and coefficient of variation (CV), were calculated for all quantitative traits. To quantify the richness and evenness of phenotypic diversity, the Shannon–Weiner diversity index (H′) was computed based on a standardized grading method. The phenotypic data for each trait were classified into 10 distinct grades based on the population mean ($\overline{X}$) and standard deviation (σ). Grade 1 included values $< (\overline{X} - 2\sigma)$, and Grade 10 included values $\geq (\overline{X} + 2\sigma)$, with intermediate grades (2 to 9) separated by intervals of 0.5σ. The diversity index was calculated as:

$$H' = -\sum_{i=1}^{n} P_i \ln P_i \quad (1)$$

where n is the number of grades (n = 10) and $P_i$ is the proportion of accessions belonging to the i-th grade.

#### 2.4.2. Correlation Analysis and Random Forest (RF) Feature Importance

Spearman rank correlation was used to characterize pairwise associations among phenotypic traits and to identify potential information overlap among morphologically related variables. Random Forest regression was then used to assess the relative predictive importance of the eight candidate traits for sugar content and root yield separately. The

dataset was split into fixed training (80%) and independent test (20%) subsets, and response-specific hyperparameters were optimized within the training subset using repeated five-fold cross-validation. Final models used 1000 trees; the optimized parameters were mtry = 1, nodesize = 5, and maxnodes = 50 for sugar content, and mtry = 1, nodesize = 20, and maxnodes = 20 for root yield. Model performance was evaluated using $R^2$, RMSE, MAE, OOB performance, and the independent test set. Permutation importance was quantified using %IncMSE, and the stability of feature rankings was assessed using 200 bootstrap resamples based on median rank, interquartile range, and the frequencies with which each trait ranked among the top three and top five predictors. Because the sugar-content model showed limited predictive performance, its RF importance ranking was interpreted cautiously and used only as supplementary evidence for indicator selection.

#### 2.4.3. Multivariate Analysis and Hierarchical Clustering

Following Z score normalization, Principal Component Analysis was conducted to elucidate intrinsic trait synergies and reduce dimensionality. Ward's hierarchical clustering based on Euclidean distance was subsequently applied to classify the germplasms into three functional typologies: Balanced, High-Sugar, and High-Yield. Prior to comparisons among the three typologies, the distributional characteristics of the quantitative traits were examined. Because several traits showed substantial departures from normality, the assumptions required for conventional parametric ANOVA-based comparisons were not adequately satisfied. Therefore, overall differences in core agronomic traits among the three typologies were evaluated using the Kruskal–Wallis test, followed by pairwise Wilcoxon rank-sum tests for post hoc comparisons. *p*-values were adjusted using the Benjamini–Hochberg method to account for multiple comparisons. Phenotypic distributions and adjusted pairwise significance levels were visualized using boxplots.

#### 2.4.4. Comprehensive Evaluation Framework

A data-informed RF–TOPSIS framework was used to rank the sugar beet accessions based on the five retained indicators. Negative RF permutation importance values (%IncMSE) were truncated to zero and normalized separately within the sugar-content and root-yield models. The two normalized importance profiles were then combined using the mean $R^2$ from the final repeated five-fold cross-validation as response-level reliability weights, yielding criterion weights of 0.220 for canopy width, 0.240 for SPAD, 0.242 for leaf length, 0.226 for plant height, and 0.072 for lower leaf angle. Canopy width, SPAD, leaf length, and plant height were treated as benefit criteria, whereas lower leaf angle was treated as a cost criterion. After vector normalization and weighting, the relative closeness coefficient ($C_i$) to the positive ideal solution was calculated, with larger $C_i$ values indicating a higher comprehensive ranking. Ranking sensitivity was assessed using equal weights, root-yield RF weights only, sugar-content RF weights only, and an unadjusted 1:1 combination of the two normalized RF importance profiles. In addition, 1000 Monte Carlo simulations were conducted at each of two perturbation levels ($\pm$10% and $\pm$20%) by independently perturbing and renormalizing the baseline criterion weights. Ranking stability was evaluated using Spearman rank correlation and Top-10 and Top-20 overlap relative to the baseline ranking.

#### 2.4.5. Statistical Software

All analyses and visualizations were conducted in R version 4.6.0 (R Foundation for Statistical Computing, Vienna, Austria) using tidyverse (version 2.0.0) [16], randomForest (version 4.7-1.2) [17], FactoMineR (version 2.15) [18], factoextra (version 2.1.0) [19], ggcorrplot (version 0.3.0) [20], ggplot2 (version 4.0.0) [21], patchwork (version 1.3.2) [22], rstatix

(version 0.7.3) [23], and ggpubr (version 0.6.3) [24]. The RF-TOPSIS ranking and sensitivity analyses were implemented using custom R scripts.

## 3. Results

### *3.1. Extensive Phenotypic Variation Among the Accessions*

Analysis of the 216 sugar beet germplasm accessions during the taproot expansion stage revealed substantial variation in measured phenotypic traits (Table 2). The coefficient of variation (CV) across the 11 measured quantitative traits ranged from 8.53% to 48.92%. Traits associated with biomass partitioning and yield exhibited the highest variability, with the R/S Ratio (CV = 48.92%) and Root Yield (CV = 34.44%) showing the greatest divergence, indicating immense potential for genetic improvement. Simultaneously, critical quality and physiological traits, such as Sugar Content (CV = 13.23%) and SPAD (CV = 13.72%), also demonstrated substantial variation.

**Table 2.** Descriptive statistics and genetic diversity analysis of quantitative traits in 216 sugar beet accessions.

| Trait | Mean ± SD | Range | CV (%) | Genetic Diversity (H′) |
|---|---|---|---|---|
| Root Yield (kg plant$^{-1}$) | 1.25 ± 0.43 | 0.41–2.61 | 34.44 | 2.04 |
| Sugar Content (%) | 12.19 ± 1.61 | 6.37–16.75 | 13.23 | 2.00 |
| R/S Ratio | 1.84 ± 0.90 | 0.43–6.54 | 48.92 | 1.94 |
| Lower Leaf Angle (°) | 63.36 ± 5.40 | 45.68–79.45 | 8.53 | 2.05 |
| Upper Leaf Angle (°) | 23.44 ± 3.03 | 17.28–35.03 | 12.95 | 2.02 |
| Canopy Width (cm) | 77.41 ± 9.65 | 56.65–110.75 | 12.46 | 2.09 |
| Plant Height (cm) | 63.94 ± 7.32 | 39.00–82.55 | 11.45 | 2.02 |
| Leaf Number | 27.19 ± 4.32 | 18.00–41.00 | 15.87 | 2.02 |
| Leaf Length (cm) | 26.24 ± 2.26 | 21.43–33.02 | 8.61 | 2.09 |
| Leaf Width (cm) | 16.03 ± 1.95 | 11.93–23.93 | 12.18 | 2.02 |
| SPAD | 35.57 ± 4.88 | 22.95–50.08 | 13.72 | 2.05 |

Note: SD, standard deviation; CV, coefficient of variation (calculated as SD/Mean × 100%); H′, Shannon–Weiner diversity index; SPAD, relative chlorophyll content; R/S Ratio, root-to-shoot ratio. SPAD and R/S Ratio are dimensionless indices, and Leaf Number is a count value.

Furthermore, the Shannon–Weiner diversity index (H′) provided deeper insight into the population structure. The H′ values for all traits were consistently high, ranging from 1.94 to 2.09, with an average of 2.03. Notably, despite the wide range of variation in yield traits, their diversity indices remained robust, as exemplified by Root Yield (H′ = 2.04), suggesting a balanced and normal frequency distribution across phenotypic classes rather than a skew towards extreme values. Regarding spatial canopy architecture, Upper Leaf Angle displayed not only a higher CV (12.95%) compared to Lower Leaf Angle (8.53%) but also a strong diversity index (H′ = 2.02). These values indicate greater among-accession variation in upper leaf angle than in lower leaf angle under the conditions evaluated.

### *3.2. Relationship Between Root Yield and Sugar Content*

The relationship between root yield and sugar content—the two primary determinants of economic value—was visualized to assess the potential for simultaneous improvement (Figure 1). The population exhibited a general inverse trajectory, as confirmed by a statistically significant negative correlation (Spearman's $r = -0.23$, $p < 0.001$).

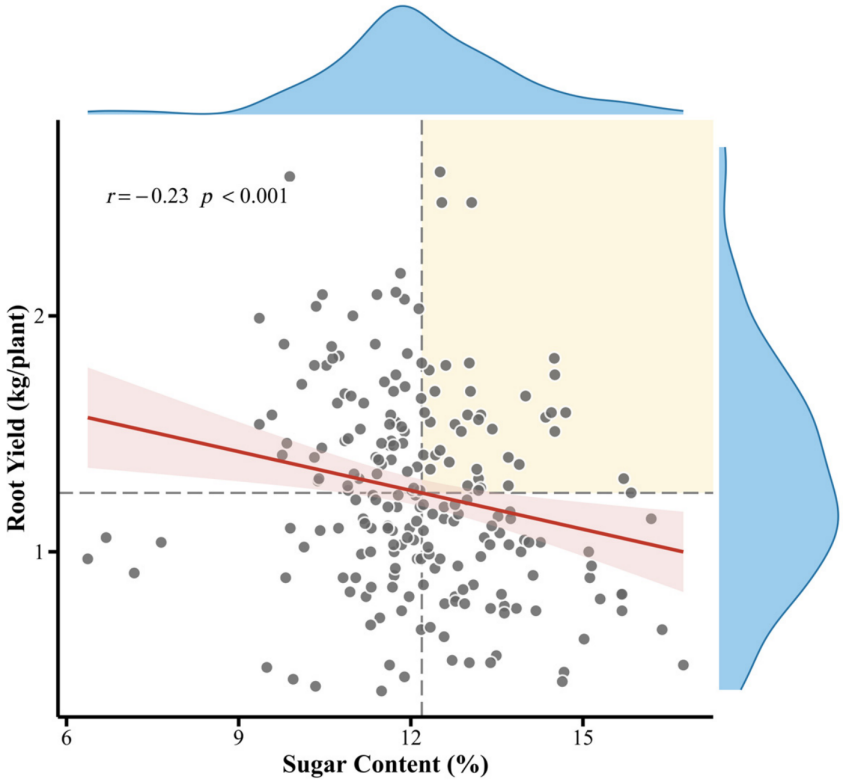


**Figure 1.** Visualization of the phenotypic relationship between root yield and sugar content in the sugar beet population ($n$ = 216). The scatter plot illustrates the bivariate distribution of individual accessions. The solid red line represents the linear regression fit with its 95% confidence interval (light red shaded band). Marginal density plots (blue curves) depict the frequency distribution of each trait. Dashed gray lines indicate the population mean values. The gold-shaded region (Quadrant I) highlights the "High-Yield & High-Sugar" target zone, identifying accessions with root yield and sugar content above their respective population means. The overall Spearman correlation was negative (Spearman's $r = -0.23$, $p < 0.001$).

### *3.3. Identification of Key Agronomic Traits via Random Forest and Correlation Analysis*

To evaluate associations between candidate phenotypic traits and sugar content and root yield, Spearman correlation analysis was combined with Random Forest (RF) regression (Figure 2). Root yield was significantly positively correlated with canopy width, leaf length, plant height, SPAD and leaf width. Sugar content was significantly negatively correlated with root yield, plant height, canopy width, and lower leaf angle. SPAD was also significantly positively correlated with canopy width (Figure 2a).

RF analysis further quantified the relative predictive importance of the eight candidate traits. For Sugar Content, Lower Leaf Angle showed the highest importance (%IncMSE = 7.57), followed by Plant Height, Leaf Length, SPAD and Upper Leaf Angle (Figure 2b). For Root Yield, Canopy Width, SPAD, Leaf Length, and Plant Height showed the largest positive importance values, whereas Upper and Lower Leaf Angles showed little positive predictive contribution (Figure 2c). Because the sugar content model showed weak predictive performance, its RF importance ranking was interpreted cautiously and used only as supplementary evidence. Based on the consistent support from root-yield correlations, RF importance, and bootstrap stability (Table S2), canopy width, SPAD, leaf length, and plant height were retained as core indicators. Lower leaf angle was additionally retained because of its significant association with sugar content and its complementary representation of leaf orientation. These five traits were therefore used as the core indicators for subsequent multi-trait evaluation.

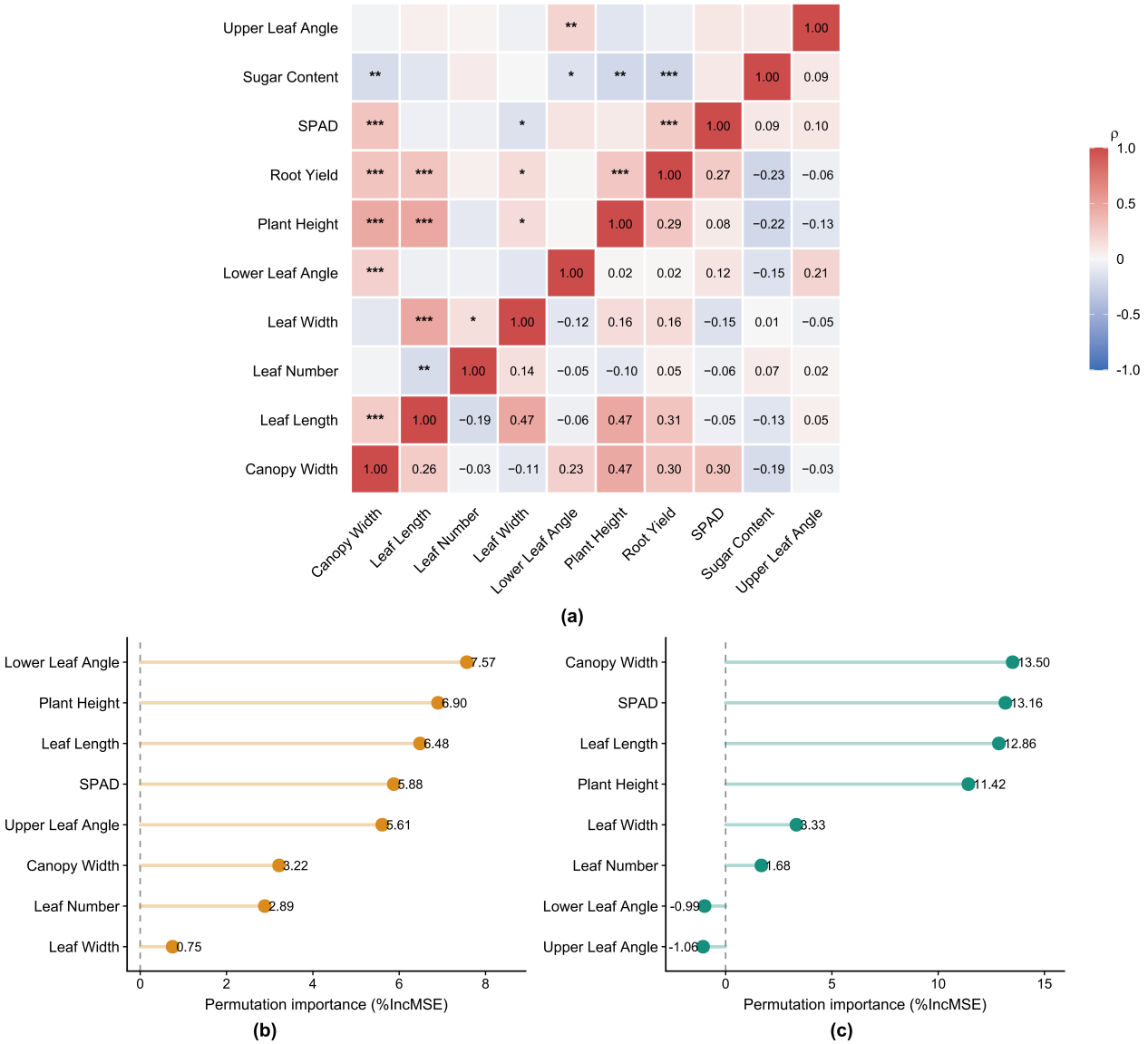


**Figure 2.** Spearman correlation structure and Random Forest (RF) feature importance of candidate phenotypic traits in sugar beet germplasm. (**a**) Spearman rank correlations among root yield, sugar content, and eight candidate phenotypic traits. Cell colors represent Spearman's correlation coefficients ($p$), ranging from blue for negative correlations to red for positive correlations, with color intensity reflecting correlation strength. Numerical correlation coefficients are shown in the lower triangle, whereas statistical significance is indicated in the upper triangle (* $p < 0.05$, ** $p < 0.01$, *** $p < 0.001$); diagonal cells represent self-correlations ($p = 1$). (**b**) RF permutation importance of the eight candidate traits for sugar content. (**c**) RF permutation importance of the eight candidate traits for root yield. Importance is expressed as the percentage increase in mean squared error (%IncMSE). Larger positive values indicate greater relative predictive contribution within the evaluated predictor set, whereas values close to or below zero indicate little or no positive predictive contribution.

### *3.4. Principal Component Analysis and Functional Typology of the Germplasm Population*

Principal Component Analysis (PCA) was used to summarize multivariate relationships among the seven selected phenotypic variables and to visualize the distribution of the sugar beet accessions in reduced-dimensional space. The first two principal components (PC1 and PC2) explained 32.0% and 17.4% of the total phenotypic variance, respectively, accounting for 49.4% of the cumulative variance. Root yield, canopy width, plant height, leaf length, and SPAD loaded predominantly in the positive direction of PC1, whereas

sugar content loaded in the opposite direction, consistent with the negative association between root yield and sugar content observed in the correlation analysis. Lower leaf angle was more strongly aligned with the positive direction of PC2, while plant height and leaf length showed comparatively stronger negative loadings on PC2.

Ward's hierarchical clustering based on Euclidean distances in the PCA coordinate space classified the 216 accessions into three phenotypic groups, while PCA was used to visualize their multivariate distribution (Figure 3). The High-Yield group was concentrated mainly toward the positive region of PC1 and was associated with higher values of yield-related canopy traits, including root yield, canopy width, plant height, leaf length, and SPAD. In contrast, the High-Sugar group was distributed predominantly toward the negative region of PC1 and showed a stronger association with sugar content. The Balanced group occupied an intermediate multivariate region between the High-Yield and High-Sugar groups and showed greater overlap with the central region of the PCA space. These patterns indicate that the three typologies represented contrasting combinations of yield, sugar content, and canopy architectural traits rather than differences in unmeasured physiological processes.

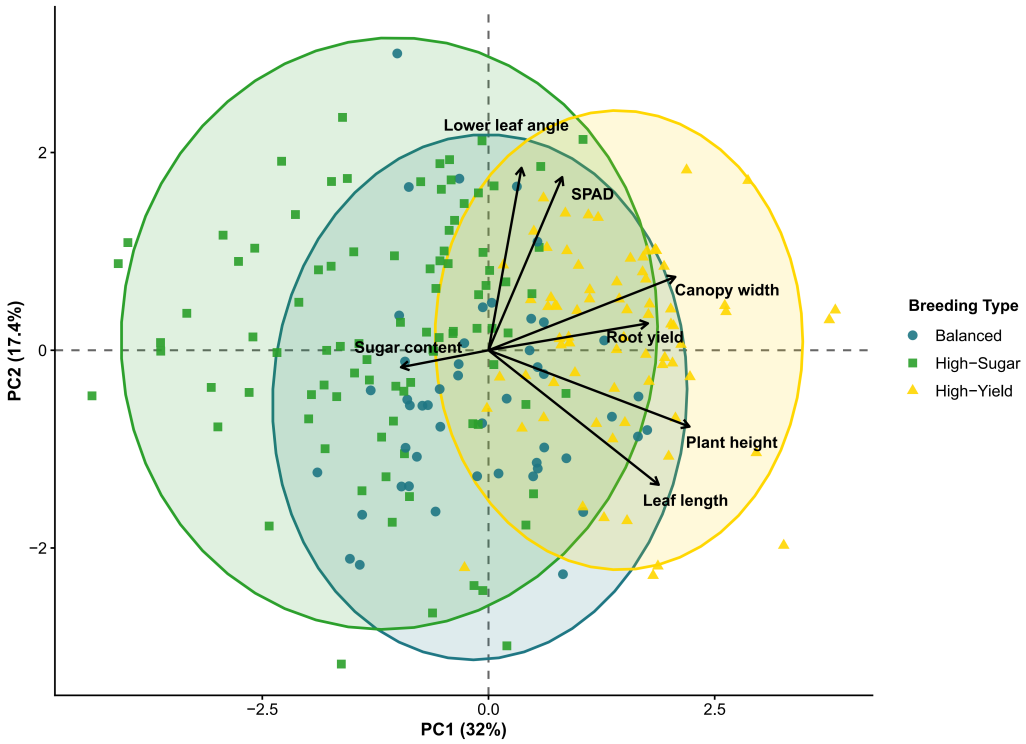


**Figure 3.** Principal Component Analysis (PCA) biplot and phenotypic typology of 216 sugar beet accessions based on seven selected phenotypic variables. Scatter points represent individual accessions classified into three groups by Ward's hierarchical clustering: Balanced (blue circles), High-Sugar (green squares), and High-Yield (yellow triangles). Shaded ellipses represent the 95% confidence regions of the three groups. Black arrows indicate the loading vectors of root yield, sugar content, canopy width, SPAD, leaf length, plant height, and lower leaf angle, with their directions reflecting relationships with the principal components and among variables. PC1 and PC2 explained 32.0% and 17.4% of the total phenotypic variance, respectively, accounting for 49.4% cumulatively.

### *3.5. Differential Analysis of Phenotypic Traits Across Sugar Beet Germplasm Typologies*

To further characterize phenotypic differences among the three germplasm typologies, the five retained core indicators, together with root yield and sugar content, were compared among the Balanced, High-Sugar, and High-Yield groups (Figure 4). Significant overall differences among typologies were detected for all seven traits. Pairwise Wilcoxon rank-

sum tests with Benjamini–Hochberg adjustment showed that the High-Yield group had significantly greater root yield than both the Balanced and High-Sugar groups, whereas the High-Sugar group had significantly higher sugar content than the other two groups. The Balanced group exhibited intermediate root yield, significantly higher than the High-Sugar group, but had the lowest sugar content among the three typologies.

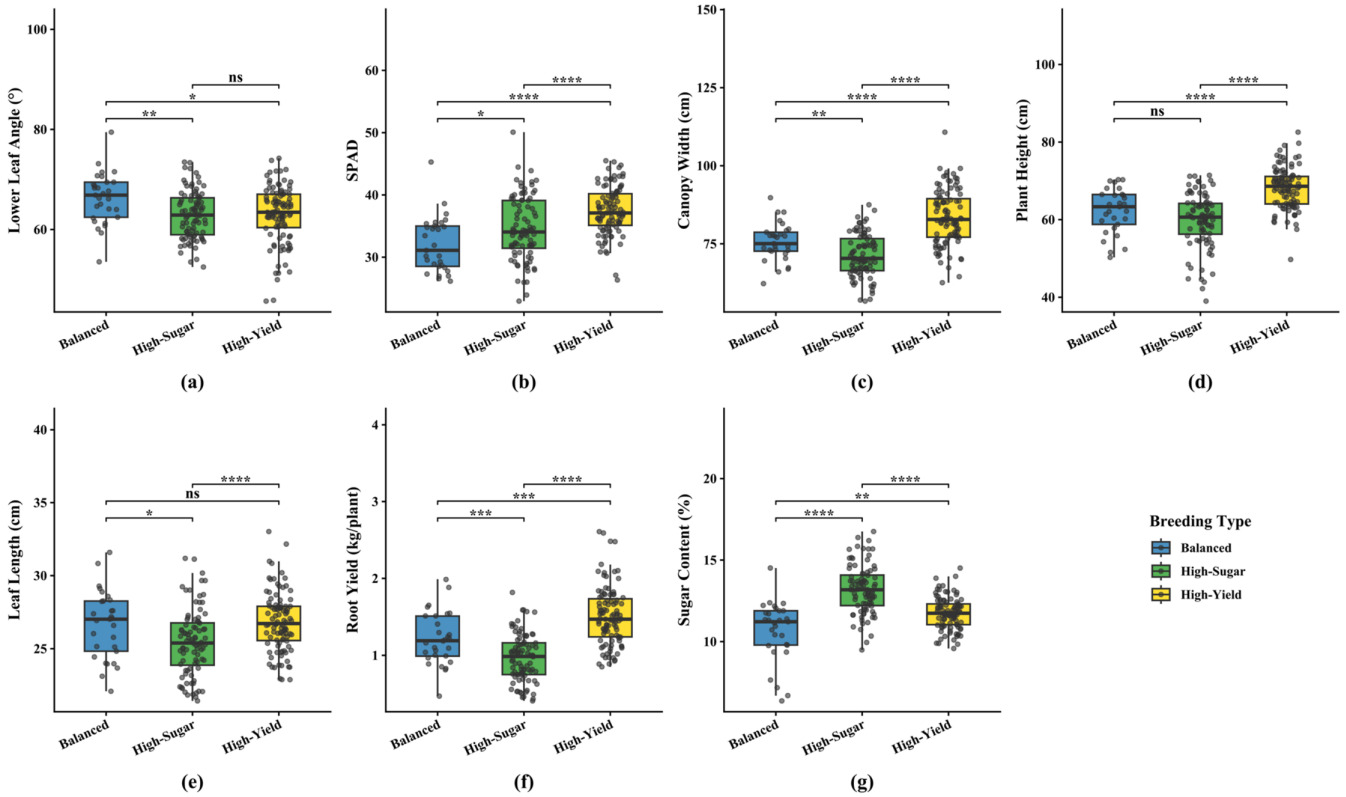


**Figure 4.** Comparative analysis of core agronomic traits across three distinct sugar beet germplasm typologies. Boxplots display the phenotypic distributions of five retained core indicators, together with root yield and sugar content: (**a**) Lower leaf angle, (**b**) SPAD, (**c**) Canopy Width, (**d**) Plant Height, (**e**) Leaf Length, (**f**) Root Yield, and (**g**) Sugar Content across the Balanced (blue), High-Sugar (green), and High-Yield (yellow) groups. The lower and upper edges of each box represent the first and third quartiles (25th and 75th percentiles), respectively, and the horizontal line within the box indicates the median. Gray dots represent individual germplasm values, with jitter applied to minimize overplotting. Overall differences among the three typologies were evaluated using the Kruskal–Wallis test, followed by pairwise Wilcoxon rank-sum tests for post hoc comparisons. *p*-values from pairwise comparisons were adjusted using the Benjamini–Hochberg method. Adjusted significance levels are indicated above the brackets (ns: not significant, * $p < 0.05$, ** $p < 0.01$, *** $p < 0.001$, **** $p < 0.0001$).

Clear differences were also observed in canopy-related traits. The High-Yield group showed significantly greater canopy width, plant height, and SPAD than the other two groups. Its leaf length was significantly greater than that of the High-Sugar group but did not differ significantly from the Balanced group. In contrast, the High-Sugar group exhibited the narrowest canopy width and shortest leaf length, while its plant height did not differ significantly from that of the Balanced group. SPAD differed significantly among all three typologies, following the order High-Yield > High-Sugar > Balanced. Lower leaf angle also differed among typologies. The Balanced group had a significantly larger lower leaf angle than both the High-Sugar and High-Yield groups, whereas no significant difference was detected between the latter two groups. Overall, these results indicate that the three typologies differed not only in root yield and sugar content but also in canopy

size, leaf chlorophyll status, leaf size, and lower-canopy orientation, providing a clear phenotypic basis for subsequent multi-trait evaluation.

### *3.6. Comprehensive Evaluation and Screening of Elite Sugar Beet Germplasms Based on Multi-Source Phenotypic Traits*

By integrating the performance-adjusted RF-derived weights with the TOPSIS framework, relative closeness coefficients ($C_i$) were calculated for all 216 sugar beet accessions to establish a comprehensive ranking. The top 20 accessions and their corresponding trait values are presented in Table 3. All top 20 accessions belonged to the High-Yield functional group. BV82 ranked first, followed by BV176, BV200, BV183, and BV144. Among the top 20 accessions, 16 originated from the Netherlands, three originated from Germany, and one originated from China.

**Table 3.** Top 20 sugar beet accessions ranked by the performance-adjusted RF–TOPSIS evaluation framework.

| Accession ID | Functional Group | Origin | Root Yield | Sugar Content | SPAD | Plant Height | Canopy Width | Leaf Length | Lower Leaf Angle | $C_i$ | Rank |
|---|---|---|---|---|---|---|---|---|---|---|---|
| BV82 | High-Yield | Netherlands | 1.66 | 14.00 | 42.58 | 74.75 | 88.28 | 27.79 | 64.76 | 0.6799 | 1 |
| BV176 | High-Yield | Germany | 1.26 | 12.16 | 45.50 | 70.08 | 81.15 | 29.83 | 63.45 | 0.6701 | 2 |
| BV200 | High-Yield | China | 1.02 | 12.30 | 36.20 | 76.60 | 94.29 | 33.02 | 68.41 | 0.6692 | 3 |
| BV183 | High-Yield | Germany | 1.58 | 11.65 | 41.58 | 70.58 | 91.04 | 27.83 | 71.68 | 0.6646 | 4 |
| BV144 | High-Yield | Netherlands | 1.46 | 9.84 | 35.58 | 74.45 | 99.13 | 32.16 | 67.03 | 0.6602 | 5 |
| BV137 | High-Yield | Netherlands | 2.10 | 11.74 | 35.80 | 79.15 | 96.60 | 29.78 | 70.81 | 0.6559 | 6 |
| BV186 | High-Yield | Germany | 1.24 | 11.78 | 42.48 | 64.30 | 92.45 | 28.36 | 69.8 | 0.6480 | 7 |
| BV146 | High-Yield | Netherlands | 1.66 | 10.96 | 41.43 | 69.73 | 96.91 | 25.59 | 69.43 | 0.6479 | 8 |
| BV102 | High-Yield | Netherlands | 1.58 | 12.99 | 41.35 | 69.10 | 91.66 | 26.93 | 66.65 | 0.6415 | 9 |
| BV119 | High-Yield | Netherlands | 1.88 | 11.30 | 37.33 | 68.03 | 110.75 | 26.08 | 68.04 | 0.6365 | 10 |
| BV143 | High-Yield | Netherlands | 1.33 | 11.01 | 35.78 | 76.00 | 96.15 | 28.42 | 73.36 | 0.6317 | 11 |
| BV97 | High-Yield | Netherlands | 1.34 | 11.94 | 36.40 | 76.30 | 94.00 | 27.9 | 58.69 | 0.6315 | 12 |
| BV149 | High-Yield | Netherlands | 1.41 | 12.43 | 44.78 | 61.23 | 97.44 | 24.75 | 73.48 | 0.6296 | 13 |
| BV115 | High-Yield | Netherlands | 1.67 | 10.85 | 38.05 | 69.98 | 90.35 | 29.84 | 68.94 | 0.6258 | 14 |
| BV87 | High-Yield | Netherlands | 1.14 | 12.58 | 39.93 | 72.20 | 85.44 | 27.71 | 65.70 | 0.6235 | 15 |
| BV105 | High-Yield | Netherlands | 1.68 | 13.04 | 39.65 | 74.33 | 84.29 | 28.15 | 65.03 | 0.6231 | 16 |
| BV129 | High-Yield | Netherlands | 1.82 | 10.64 | 34.33 | 82.55 | 87.45 | 30.20 | 74.23 | 0.6217 | 17 |
| BV127 | High-Yield | Netherlands | 1.10 | 9.90 | 37.10 | 79.70 | 85.21 | 27.83 | 62.71 | 0.6162 | 18 |
| BV130 | High-Yield | Netherlands | 1.22 | 11.04 | 42.63 | 71.03 | 82.41 | 25.53 | 69.08 | 0.6108 | 19 |
| BV96 | High-Yield | Netherlands | 2.07 | 11.89 | 40.58 | 68.83 | 85.84 | 27.39 | 61.66 | 0.6108 | 20 |

Note: Functional Group denotes the germplasm typology assigned by Ward's hierarchical clustering. Origin indicates the geographical source of each accession. $C_i$ represents the TOPSIS relative closeness coefficient to the positive ideal solution, calculated as $C_i = D_i^- / (D_i^+ + D_i^-)$, where $D_i^+$ and $D_i^-$ are the Euclidean distances from the positive and negative ideal solutions, respectively. Larger $C_i$ values indicate closer proximity to the defined multi-trait ideal and therefore a higher comprehensive ranking. Trait units are as follows: Root Yield (kg plant$^{-1}$); Sugar Content (%); SPAD; Plant Height, Canopy Width, and Leaf Length (cm); Lower Leaf Angle (°).

Ranking sensitivity analyses further indicated that the overall ordering was generally stable across alternative weighting schemes (Table S3). Spearman rank correlations with the baseline ranking were 0.978 under equal weights, 0.996 under root-yield RF weights only, and 0.995 under the unadjusted combined RF weighting scheme, whereas the sugar-content RF-only scheme showed lower agreement. Monte Carlo perturbations of the baseline weights yielded mean rank correlations of 0.998 and 0.992 under ±10% and ±20% perturbations, respectively, with mean Top-20 overlaps of 19.16 and 18.05 accessions. These results indicate that the overall ranking was generally stable to moderate changes in criterion weights.

## 4. Discussion

### *4.1. 3D Canopy Architecture and Spatial Ideotype Optimization*

Modern agricultural practices increasingly emphasize canopy optimization as a means of improving population-level productivity [2,5,6]. Canopy architecture determines the spatial distribution of foliage and therefore affects light interception, within-canopy light gradients, and radiation use efficiency (RUE), making plant architecture an important target in crop ideotype breeding [7–10]. The "smart canopy" concept suggests that optimal canopy performance may depend on coordinated variation in leaf orientation and canopy structure across different canopy layers rather than uniform modification of a single trait [5]. In sugar beet, previous studies have similarly shown that canopy angle influences light interception, RUE, biomass partitioning, and sugar yield [6,7,11].

Our results support this multidimensional view of canopy architecture. Canopy width, plant height, leaf length, and SPAD were positively associated with root yield and showed relatively high predictive importance in the RF analysis, whereas lower leaf angle provided complementary information related to sugar content. These relationships suggest that favorable canopy performance may emerge from coordinated variation in horizontal canopy expansion, vertical development, leaf size, chlorophyll status, and lower-canopy orientation rather than from optimization of any single architectural trait. The High-Yield group further illustrated this pattern. These accessions exhibited greater canopy width, plant height, and SPAD than the other typologies, together with higher root yield. A broader and taller canopy may increase the spatial capacity for foliage deployment and light interception, while higher SPAD readings indicate greater leaf greenness at the time of measurement. In combination, these traits may influence canopy light distribution [25–27]. However, canopy light interception, photosynthetic rates, and RUE were not directly measured in the present study; therefore, this interpretation should be regarded as a testable physiological hypothesis rather than a directly demonstrated mechanism.

Lower leaf angle may represent an additional architectural dimension that is not fully captured by canopy size alone. Its association with sugar content, together with the relatively weak predictive contribution of leaf angles to root yield, suggests that lower-canopy orientation may influence canopy function differently from traits primarily associated with biomass production. One possibility is that variation in lower-leaf orientation alters light penetration and the balance of photosynthetic activity among canopy layers, thereby affecting the relationship between vegetative growth and sucrose accumulation. Direct measurements of vertical light profiles and canopy photosynthesis would be required to evaluate this possibility. Because all accessions were evaluated under a single planting configuration, the present study identifies architectural characteristics associated with performance under the tested spacing only. It does not directly test adaptation to high-density cultivation, density tolerance, or the stability of these trait–performance relationships across planting densities. Multi-density field experiments will be required to test the generality of these relationships and quantify genotype × density interactions.

### *4.2. Possible Physiological Explanations for the Yield and Quality Trade-Off*

Root yield and sugar content showed a significant negative association across the 216 accessions, indicating a phenotypic trade-off between root biomass production and sucrose concentration. Similar negative relationships have been reported previously in sugar beet [28]. From a physiological perspective, this pattern may arise when rapid taproot biomass accumulation is not accompanied by a proportional increase in sucrose deposition, leading to dilution of sugar concentration. Variation in assimilate allocation between structural growth and sucrose storage may further contribute to the observed relationship [29,30]. Experimental evidence from sugar beet taproot tissue has also shown

that turgor can influence sucrose transport, highlighting the potential importance of sink regulation [13]. However, because the relevant physiological processes, including carbon assimilation, assimilate partitioning, sucrose transport, and source–sink dynamics, were not directly measured, these explanations should be regarded as hypotheses rather than demonstrated causal mechanisms.

The PCA and hierarchical clustering analyses nevertheless revealed clear phenotypic differentiation among the evaluated germplasms. The High-Yield group was associated with higher root yield, plant height, canopy width, and SPAD, whereas the High-Sugar group was characterized by higher sugar content and relatively smaller canopy dimensions. The Balanced group occupied an intermediate multivariate position between the High-Yield and High-Sugar groups. These patterns suggest that the yield–quality trade-off may be associated with different combinations of canopy development and storage-related traits rather than with a single morphological determinant.

The positive association between SPAD and canopy width is also noteworthy. Canopy expansion and biomass accumulation are closely linked to plant nitrogen demand, and sugar beet studies based on critical nitrogen dilution relationships have shown that plant nitrogen concentration changes systematically with biomass accumulation [31,32]. In the present study, accessions with wider canopies also tended to have higher SPAD readings. This association suggests that canopy size and leaf greenness varied together among accessions, but it does not establish differences in nitrogen acquisition, photosynthetic capacity, or senescence. Taken together, these phenotypic patterns may reflect different configurations associated with the yield–quality trade-off. Whether they are underpinned by differences in carbon assimilation, assimilate partitioning, nitrogen economy, or source–sink dynamics will require direct physiological investigation.

Several limitations should be considered when interpreting the present findings. First, the experiment used a single planting configuration; therefore, the observed trait–performance relationships cannot establish adaptation to high-density cultivation or their stability across plant densities. Second, the study did not directly quantify canopy light interception, gas exchange and carbon assimilation, radiation use efficiency, assimilate partitioning, source–sink dynamics, sucrose transport, or nitrogen acquisition. Consequently, the physiological interpretations proposed above should be regarded as literature-informed hypotheses rather than mechanisms demonstrated by the present experiment. Future work should combine multi-density and multi-environment trials with direct physiological measurements to test these hypotheses and determine whether the identified canopy trait combinations are consistently associated with favorable performance.

### *4.3. Multi-Trait Germplasm Evaluation and Breeding Applications*

The evaluation of complex germplasm resources requires integration of multiple traits because individual variables generally represent only one component of overall plant performance. Conventional correlation analysis is useful for identifying pairwise relationships, but it may not fully represent nonlinear and multivariate associations among canopy traits, yield, and sugar content. Machine-learning approaches can complement conventional statistical methods by evaluating predictive relationships among multiple interacting variables [33–35].

In the present study, Spearman correlation analysis and RF regression jointly identified five complementary indicators, including canopy width, SPAD, leaf length, plant height, and lower leaf angle, for subsequent multi-trait evaluation. Similar machine-learning approaches have been used to integrate high-dimensional phenotypic information and identify informative predictors for crop breeding and yield prediction [36]. Importantly, the predictive performance of the two RF models was not equivalent. The root-yield

model provided stronger predictive information, whereas the sugar-content model showed comparatively weak predictive performance. Accordingly, sugar-content RF importance was treated only as supplementary evidence rather than as a stand-alone basis for feature selection. The RF-derived importance profiles were subsequently incorporated into TOPSIS using performance-adjusted response weights, allowing the five retained indicators to be integrated while accounting for differences in model performance.

The resulting RF-TOPSIS ranking identified BV82 as the highest-ranked accession, followed by BV176, BV200, BV183, and BV144. All top 20 accessions belonged to the High-Yield functional group; among them, 16 originated from the Netherlands, three originated from Germany, and one originated from China. These distributions indicate that the current weighting scheme preferentially selected accessions combining strong yield-associated canopy characteristics within the evaluated panel. However, the geographical composition of the top-ranked subset should not be interpreted as evidence of inherent genetic superiority among origins. Sensitivity analyses further indicated that the overall ranking was generally stable under alternative weighting schemes and moderate perturbations of criterion weights. Rank correlations remained high under equal weighting, root-yield RF weighting, and the unadjusted combined RF weighting scheme, while Monte Carlo perturbations of $\pm 10\%$ and $\pm 20\%$ also maintained substantial agreement with the baseline ranking. This consistency indicates that the ranking was not highly dependent on small changes in the weighting structure. Nevertheless, ranking stability should be distinguished from biological validation: methodological consistency within the present dataset does not by itself demonstrate superior performance across environments or breeding populations.

Overall, the performance-adjusted RF-TOPSIS framework provides a quantitative approach for integrating complementary canopy traits associated with root yield and sugar content. Rather than replacing conventional breeding evaluation, the framework can be used to prioritize candidate accessions for subsequent field testing and genetic analysis. In this context, the top-ranked materials provide candidate resources for multi-environment validation, genome-wide association studies, and genomic selection aimed at improving the coordination of canopy architecture, root yield, and sugar content.

## 5. Conclusions

A systematic evaluation of 216 sugar beet accessions revealed substantial phenotypic diversity in canopy architecture, root yield, and sugar content under the tested planting condition. By integrating Spearman correlation analysis with Random Forest regression, five complementary indicators, including canopy width, SPAD, leaf length, plant height, and lower leaf angle, were retained for multi-trait evaluation. Principal Component Analysis and hierarchical clustering further differentiated the germplasm population into High-Yield, High-Sugar, and Balanced phenotypic typologies, reflecting distinct combinations of yield, sugar content, and canopy traits.

The performance-adjusted RF-TOPSIS framework provided a quantitative ranking of the 216 accessions based on these five indicators, with BV82 achieving the highest relative closeness coefficient. Sensitivity analyses indicated that the overall ranking was generally stable under alternative weighting schemes and moderate perturbations of criterion weights. These results identify candidate canopy traits and germplasm resources for further evaluation and breeding applications but should be interpreted as phenotypic associations under the tested planting condition. Further multi-density, multi-environment, and physiologically informed validation is required to assess the broader applicability of these trait combinations and accession rankings.

**Supplementary Materials:** The following supporting information can be downloaded at https://www.mdpi.com/article/10.3390/agronomy16191974/s1, Table S1: The basic information of maize germplasm for testing; Table S2: Bootstrap stability of RF feature rankings; Table S3: Sensitivity analysis of the RF-TOPSIS ranking.

**Author Contributions:** Conceptualization, R.S. and K.S.; methodology, Z.Y.; software, R.S.; validation, R.W., Z.Y. and Y.L.; formal analysis, Y.L.; investigation, Y.L.; resources, R.W.; data curation, Y.L.; writing—original draft preparation, R.S.; writing—review and editing, K.S. and Z.Y.; visualization, R.S.; supervision, R.W.; project administration, Z.Y.; funding acquisition, K.S. All authors have read and agreed to the published version of the manuscript.

**Funding:** This research was funded by the Scientific Research Start-up Fund for Industrial Technology Innovation Program of IMAST, grant number 2024RCYJ04004 and 2024RCYJ04006.

**Data Availability Statement:** Data is contained within the article.

**Conflicts of Interest:** The authors declare no conflicts of interest.

## Abbreviations

The following abbreviations are used in this manuscript:

| | |
|---|---|
| RF | Random Forest |
| SPAD | Relative Chlorophyll Content |
| PCA | Principal Component Analysis |
| RF-TOPSIS | Random Forest—Technique for Order Preference by Similarity to Ideal Solution |
| R/S Ratio | Root-to-Shoot Ratio |
| DAS | Days After Sowing |

## References

1. Tilman, D.; Balzer, C.; Hill, J.; Befort, B.L. Global Food Demand and the Sustainable Intensification of Agriculture. *Proc. Natl. Acad. Sci. USA* **2011**, *108*, 20260–20264. [CrossRef] [PubMed]
2. Koch, H.; Grunwald, D.; Hoffmann, C.M. Sugar Beet Response to Varied Plant Populations—Current and Historic Trial Results. *Agron. J.* **2026**, *118*, e70350. [CrossRef]
3. Reinsdorf, E.; Koch, H.-J.; Loel, J.; Hoffmann, C.M. Yield of Bolting Winter Beet (*Beta vulgaris* L.) as Affected by Plant Density, Genotype and Environment. *Eur. J. Agron.* **2014**, *54*, 1–8. [CrossRef]
4. Varga, I.; Lončarić, Z.; Kristek, S.; Kulundžić, A.M.; Rebekić, A.; Antunović, M. Sugar Beet Root Yield and Quality with Leaf Seasonal Dynamics in Relation to Planting Densities and Nitrogen Fertilization. *Agriculture* **2021**, *11*, 407. [CrossRef]
5. Tian, J.; Wang, C.; Chen, F.; Qin, W.; Yang, H.; Zhao, S.; Xia, J.; Du, X.; Zhu, Y.; Wu, L.; et al. Maize Smart-Canopy Architecture Enhances Yield at High Densities. *Nature* **2024**, *632*, 576–584. [CrossRef] [PubMed]
6. Chen, H.; Zhang, M.; Xiao, S.; Wang, Q.; Cai, Z.; Dong, Q.; Feng, P.; Shao, K.; Ma, Y. Quantitative Analysis and Planting Optimization of Multi-Genotype Sugar Beet Plant Types Based on 3D Plant Architecture. *Comput. Electron. Agric.* **2024**, *225*, 109231. [CrossRef]
7. Tillier, L.C.; Murchie, E.H.; Sparkes, D.L. Does Canopy Angle Influence Radiation Use Efficiency of Sugar Beet? *Field Crops Res.* **2023**, *293*, 108841. [CrossRef]
8. Mantilla-Perez, M.B.; Salas Fernandez, M.G. Differential Manipulation of Leaf Angle throughout the Canopy: Current Status and Prospects. *J. Exp. Bot.* **2017**, *68*, 5699–5717. [CrossRef] [PubMed]
9. Burgess, A.J.; Retkute, R.; Herman, T.; Murchie, E.H. Exploring Relationships between Canopy Architecture, Light Distribution, and Photosynthesis in Contrasting Rice Genotypes Using 3D Canopy Reconstruction. *Front. Plant Sci.* **2017**, *8*, 734. [CrossRef] [PubMed]
10. Zhu, X.-G.; Long, S.P.; Ort, D.R. Improving Photosynthetic Efficiency for Greater Yield. *Annu. Rev. Plant Biol.* **2010**, *61*, 235–261. [CrossRef] [PubMed]
11. Hoffmann, C.M. Importance of Canopy Closure and Dry Matter Partitioning for Yield Formation of Sugar Beet Varieties. *Field Crops Res.* **2019**, *236*, 75–84. [CrossRef]
12. Hoffmann, C.M.; Kenter, C. Yield Potential of Sugar Beet—Have We Hit the Ceiling? *Front. Plant Sci.* **2018**, *9*, 289. [CrossRef] [PubMed]

13. Wyse, R.E.; Zamski, E.; Tomos, A.D. Turgor Regulation of Sucrose Transport in Sugar Beet Taproot Tissue. *Plant Physiol.* **1986**, *81*, 478–481. [CrossRef] [PubMed]
14. Fugate, K.K.; Eide, J.D.; Martins, D.N.; Grusak, M.A.; Deckard, E.L.; Finger, F.L. Colocalization of Sucrose Synthase Expression and Sucrose Storage in the Sugarbeet Taproot Indicates a Potential Role for Sucrose Catabolism in Sucrose Accumulation. *J. Plant Physiol.* **2019**, *240*, 153016. [CrossRef] [PubMed]
15. Liu, D.; Tan, W.; Wang, H.; Li, W.; Fu, J.; Li, J.; Zhou, Y.; Lin, M.; Xing, W. Genetic Diversity and Genome-Wide Association Study of 13 Agronomic Traits in 977 *Beta vulgaris* L. Germplasms. *BMC Genom.* **2023**, *24*, 413. [CrossRef] [PubMed]
16. Wickham, H.; Averick, M.; Bryan, J.; Chang, W.; McGowan, L.; François, R.; Grolemund, G.; Hayes, A.; Henry, L.; Hester, J.; et al. Welcome to the Tidyverse. *J. Open Source Softw.* **2019**, *4*, 1686. [CrossRef]
17. Liaw, A.; Wiener, M. Classification and Regression by randomForest. *R News* **2002**, *2*, 18–22.
18. Lê, S.; Josse, J.; Husson, F. FactoMineR: An *R* Package for Multivariate Analysis. *J. Stat. Softw.* **2008**, *25*, 1–18. [CrossRef]
19. Kassambara, A.; Mundt, F. Factoextra: Extract and Visualize the Results of Multivariate Data Analyses. R Package Version 2.1.0. 2026. Available online: https://cran.r-project.org/web/packages/factoextra/index.html (accessed on 3 October 2026).
20. Kassambara, A. Ggcorrplot: Visualization of a Correlation Matrix Using 'Ggplot2'. R Package Version 0.3.0. 2026. Available online: https://cran.r-project.org/web/packages/ggcorrplot/index.html (accessed on 3 October 2026).
21. Wickham, H. *Ggplot2: Elegant Graphics for Data Analysis*; Use R!; Springer: Cham, Switzerland, 2016; ISBN 978-3-319-24275-0. [CrossRef]
22. Pedersen, T.L. Patchwork: The Composer of Plots. R Package Version 1.3.2. 2025. Available online: https://cran.r-project.org/web/packages/patchwork/index.html (accessed on 3 October 2026).
23. Kassambara, A. Rstatix: Pipe-Friendly Framework for Basic Statistical Tests. R Package Version 0.7.3. 2026. Available online: https://cran.r-project.org/web/packages/rstatix/index.html (accessed on 3 October 2026).
24. Kassambara, A. Ggpubr: "ggplot2" Based Publication Ready Plots. R Package Version 0.6.3. 2026. Available online: https://cran.r-project.org/web/packages/ggpubr/index.html (accessed on 3 October 2026).
25. Ort, D.R.; Merchant, S.S.; Alric, J.; Barkan, A.; Blankenship, R.E.; Bock, R.; Croce, R.; Hanson, M.R.; Hibberd, J.M.; Long, S.P.; et al. Redesigning Photosynthesis to Sustainably Meet Global Food and Bioenergy Demand. *Proc. Natl. Acad. Sci. USA* **2015**, *112*, 8529–8536. [CrossRef] [PubMed]
26. Long, S.P.; Zhu, X.; Naidu, S.L.; Ort, D.R. Can Improvement in Photosynthesis Increase Crop Yields? *Plant Cell Environ.* **2006**, *29*, 315–330. [CrossRef] [PubMed]
27. Song, Q.; Wang, Y.; Qu, M.; Ort, D.R.; Zhu, X. The Impact of Modifying Photosystem Antenna Size on Canopy Photosynthetic Efficiency—Development of a New Canopy Photosynthesis Model Scaling from Metabolism to Canopy Level Processes. *Plant Cell Environ.* **2017**, *40*, 2946–2957. [CrossRef] [PubMed]
28. Fasahat, P.; Aghaeezadeh, M.; Hosseinpour, M.; Sadeghzadeh Hemayati, S. Correlation between Root Weight and Sugar Content; Do We Have to Continue Traditional Hypothesis? *Plant Physiol. Rep.* **2021**, *26*, 188–191. [CrossRef]
29. Sonnewald, U.; Fernie, A.R. Next-Generation Strategies for Understanding and Influencing Source–Sink Relations in Crop Plants. *Curr. Opin. Plant Biol.* **2018**, *43*, 63–70. [CrossRef] [PubMed]
30. Braun, D.M.; Wang, L.; Ruan, Y.-L. Understanding and Manipulating Sucrose Phloem Loading, Unloading, Metabolism, and Signalling to Enhance Crop Yield and Food Security. *J. Exp. Bot.* **2014**, *65*, 1713–1735. [CrossRef] [PubMed]
31. Wang, Y.; Yan, F.; Fan, J.; Zhang, F. Optimization of Irrigation Amount and Nitrogen Rate of Drip-Fertigated Sugar Beet Based on Sugar Yield, Nitrogen Use Efficiency, and Critical Nitrogen Dilution Curve in the Arid Southern Xinjiang of China. *Plants* **2025**, *14*, 2055. [CrossRef] [PubMed]
32. Zhang, J.K.; Li, F.; Shi, S.D.; Yang, H.B. Construction and application of the critical nitrogen concentration dilution model of sugar beet in Inner Mongolia, China. *Acta Agron. Sin.* **2022**, *48*, 488–496. [CrossRef]
33. Maimaitijiang, M.; Sagan, V.; Sidike, P.; Hartling, S.; Esposito, F.; Fritschi, F.B. Soybean Yield Prediction from UAV Using Multimodal Data Fusion and Deep Learning. *Remote Sens. Environ.* **2020**, *237*, 111599. [CrossRef]
34. Van Klompenburg, T.; Kassahun, A.; Catal, C. Crop Yield Prediction Using Machine Learning: A Systematic Literature Review. *Comput. Electron. Agric.* **2020**, *177*, 105709. [CrossRef]
35. Chlingaryan, A.; Sukkarieh, S.; Whelan, B. Machine Learning Approaches for Crop Yield Prediction and Nitrogen Status Estimation in Precision Agriculture: A Review. *Comput. Electron. Agric.* **2018**, *151*, 61–69. [CrossRef]
36. Parmley, K.; Nagasubramanian, K.; Sarkar, S.; Ganapathysubramanian, B.; Singh, A.K. Development of Optimized Phenomic Predictors for Efficient Plant Breeding Decisions Using Phenomic-Assisted Selection in Soybean. *Plant Phenomics* **2019**, *2019*, 5809404. [CrossRef] [PubMed]


**Disclaimer/Publisher's Note:** The statements, opinions and data contained in all publications are solely those of the individual author(s) and contributor(s) and not of MDPI and/or the editor(s). MDPI and/or the editor(s) disclaim responsibility for any injury to people or property resulting from any ideas, methods, instructions or products referred to in the content.